Optically enhanced single- and multi-stacked 1.55 μm InAs/InAlGaAs/InP quantum dots for laser applications

OPEN ACCESS
IOP Publishing
Journal of Physics D: Applied Physics
J. Phys. D: Appl. Phys. **56** (2023) 285101 (8pp)
https://doi.org/10.1088/1361-6463/acc875

Optically enhanced single- and multi-stacked 1.55 μm InAs/InAlGaAs/InP quantum dots for laser applications

Xuezhe Yu[1,*], Hui Jia[1], Calum Dear, Jiajing Yuan, Huiwen Deng, Mingchu Tang and Huiyun Liu

Department of Electronic and Electrical Engineering, University College London, London WC1E 7JE, United Kingdom

E-mail: xuezhe.yu@ucl.ac.uk

Received 12 January 2023, revised 2 March 2023
Accepted for publication 28 March 2023
Published 27 April 2023

Abstract

For the development of InAs/InP quantum dot (QD) lasers for 1.55 μm telecom wavelength, there are two main challenges: (1) morphological preference for quantum dashes over QDs, and (2) generally poor size uniformity of QDs (dashes). This study addresses the issues, in synchronous, by demonstrating the improved optical properties of 1.55 μm InAs/InP QDs at room temperature with excellent reproducibility. A high-density ($\sim 4 \times 10^{10}$ cm^{-2}) dot-like morphology was initially attained via adjusting the growth parameters, *albeit* with a large full-width at half-maximum (FWHM) of $\sim$80 meV and a peak position of a wavelength longer than 1.55 μm. For improvement, the indium-flush technique was employed, which enhanced the uniformity of InAs QDs and substantially lowered the FWHM of five (single) stacked QDs to 50.9 meV (47.9 meV). This technique also blue-shifted the emission peak to 1530.2 nm (1522 nm). The InAs/InP QDs presented are appropriate for the fabrication of high-performance 1.55 μm lasers on InP (001) and, potentially, emerging light sources on the important Si (001).

Keywords: quantum dots, 1.55 μm, InAs, molecular beam epitaxy

(Some figures may appear in colour only in the online journal)

Applications in the telecommunications C-band have shown great promise for light sources made from 1.55 μm InAs quantum dots (QDs) [1, 2]. In particular, prompted by their atomic-like characteristics, their telecom-band lasers are expected to offer the benefits of low threshold current density, excellent thermal stability, and significant material modal gain with a wide range of applications such as data communications, non-invasive medical sensing, and machine vision. While progress is still being made in the development of 1.55 μm InAs/InP QDs (both InAs/InAlGaAs/InP and InAs/InGaAsP/InP QDs) [1–7], it has been relatively slow compared to that of 1.3 μm InAs/GaAs QDs systems [8–10], which have been extensively investigated for many applications over the last few decades, including, most recently, monolithically integrated lasers with Si (001) platforms [11, 12]. The challenge with InAs/InP QDs, as opposed to InAs/GaAs QDs, is that typically elongated quantum dash structures nucleated in the $[\bar{1}10]$ direction,

[1] X Z Yu and H Jia contributed equally to this work.
[*] Author to whom any correspondence should be addressed.

rather than QDs [1]. Due to their inhomogeneity, the photoluminescence (PL) spectra of quantum dashes are generally broader, which has a detrimental impact on laser performance. The anisotropic surface diffusion of indium adatoms, the reduced lattice mismatch, and the complicated strain distribution in InAs/InP systems may all be contributing factors to the emergence of quantum dashes. Despite encouraging progress toward 1.55 μm lasers based on InAs quantum dashes [13–17], significant efforts have also been undertaken to acquire InAs QDs. It has been found that morphologically preferred, round dot-like InAs/InAlGaAs QDs can be obtained via molecular beam epitaxy (MBE) growth using As_2 and/or by employing growth interruptions [4, 7], which offers a promising route to the implementation of C-band lasers on InP substrates and, potentially, on the important Si substrates.

In addition to the stringent requirements for morphology, it is recognised that the optical characteristics of InAs QDs should fulfil the following criteria if they are to be exploited as active materials for high-performance laser applications: (1) the wavelength is near 1.55 μm; (2) the full-width at half-maximum (FWHM) of the PL spectrum should be as narrow as possible, indicating that the QDs are more uniform and contribute to enhanced laser gain; (3) the PL intensity should be as strong as possible, which is a way of characterising the quality of the QD ensemble and the extent of light absorption by the surroundings close to the laser active region; and (4) the above measurements should be performed at room temperature (RT). This is because the most common environment in which lasers operate is at RT, and although lasing at RT guarantees that it will function even at low temperatures, the inverse is not necessarily true.

Thus, improving the general optical properties of morphologically optimised InAs QDs to meet the aforementioned criteria is critical. For instance, the narrow FWHM is a measure of the uniformity of QDs. In principle, a smaller FWHM may be achieved by decreasing the surface density of QDs; however, this approach is impractical for fabricating high-gain lasers. Therefore, increasing QD density (on the order of 10^{10} cm^{-2}) and QD uniformity in synchronous is necessary to maximise the optical gain of the laser. Based on the examination of these two parameters in the relevant literature, a typical FWHM value is around 70 meV at RT and seldom below 60 meV [1, 18]. This includes the results of recent work on improving the optical properties of InAs/InAlGaAs/InP QDs by double-cap growth technique via metal-organic chemical vapour deposition [6]. The FWHM of PL spectra obtained in some literature is very narrow, peaking around 1.55 μm, but measured at low temperatures (LT) with a low excitation power density of 0.2 W cm^{-2} [4, 5], which might have assisted in achieving narrower FWHM. On the other hand, it has long been well-understood that dot-like, more uniform InAs QDs can be grown on InP (311) substrates [19, 20]; nonetheless, this strategy is not preferable from the perspective of the standard laser fabrication process and photonic integrated circuits, for both of which (001) substrates are preferred, limiting the broader applicability of 1.55 μm InAs QDs.

This work demonstrates a considerable improvement in the optical characteristics of 1.55 μm InAs QDs on InP (001) at RT. To this end, first, we optimised the shape and density of InAs QDs on InP (001) substrates employing a wide range of growth conditions, including growth temperature and InAs deposition thickness. Consequently, a dot-like morphology was obtained with a density of $\sim 4 \times 10^{10}$ cm^{-2}; nevertheless, the QDs had deviated peak positions, broad FWHMs and relatively low PL intensities that severely fell short of the criteria. To improve, the QDs were subsequently subjected to the indium-flush (In-flush) technique, which increased their uniformity and narrowed the FWHM of the five (single)-stack QDs to 50.9 meV (47.9 meV). In parallel, the emission peaks were blue-shifted to 1530.2 nm (1522 nm) following the implementation of the technique.

The structures under investigation were grown on n-type InP (001) ($\pm 0.5°$) substrates by MBE equipped with a valved arsenic cracker source. The whole epitaxial growth is phosphorus-free. The substrates were initially degassed at 400 °C for 1 h in the preparation chamber, then transferred to the growth chamber, heated to 500 °C under As_2 overpressure, and held at this temperature for one minute to remove surface oxides. Figure 1 serves as the basis for the sample structures studied in this paper. Detailed descriptions of the structures of the various samples, with an emphasis on the information of the InAs QDs and the following capping layer development, will be provided where appropriate below. The buffer layers in these samples are lattice-matched to InP and consist of 500 nm $In_{0.524}Al_{0.476}As$ and 100 nm $In_{0.528}Al_{0.234}Ga_{0.238}As$. Thereafter, InAs QDs were produced in As_2 mode at 485 °C with a growth rate of 0.42 ML s^{-1} and a V/III beam equivalent pressure ratio of 18 was used. A growth interruption of 10 s was applied to facilitate the QDs formation and enhance the QDs uniformity. This was followed by 100 nm $In_{0.528}Al_{0.234}Ga_{0.238}As$ and 200 nm $In_{0.524}Al_{0.476}As$. These dots were primarily used for characterising optical properties through PL measurements with a power density of 430 W cm^{-2}. After growing an additional 100 nm of $In_{0.528}Al_{0.234}Ga_{0.238}As$, a layer of QDs was formed under the same growth condition as the previous QDs, which were used for surface morphological characterisation by atomic force microscopy (AFM).

First, we investigated how the morphology of InAs QDs was affected by depositing InAs at several thicknesses ranging from 3.5 ML to 6.4 ML. Figure 2 shows the AFM results for all deposition thicknesses, with all the samples being able to develop into the desired morphology of InAs QDs, despite differences in density. However, upon further inspection, it reveals that for thinner deposition thicknesses, such as 3.5 ML and 4 ML, large areas of quantum dashes could be seen to nucleate on the surface in addition to low-density QDs. As the thickness of InAs increases, the QD density increases whilst the quantum dashes become invisible, suggesting that the development of quantum dashes is impeded in the latter stages of growth. Therefore, it follows that the whole growth process operates in two distinct modes. The

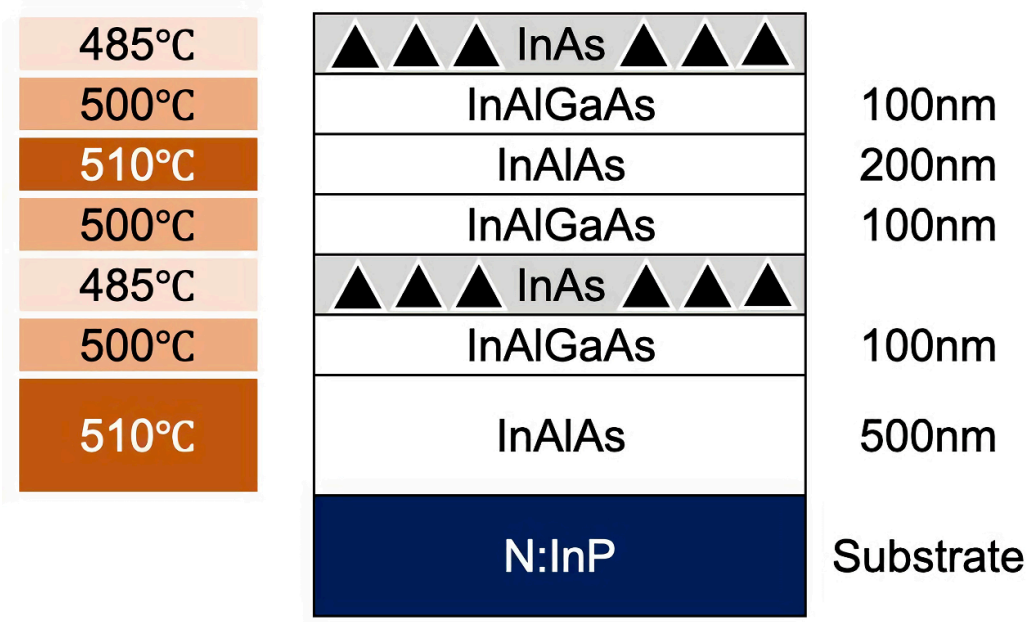

Figure 1. Typical growth structure of InAs/InP QDs implemented in this study.

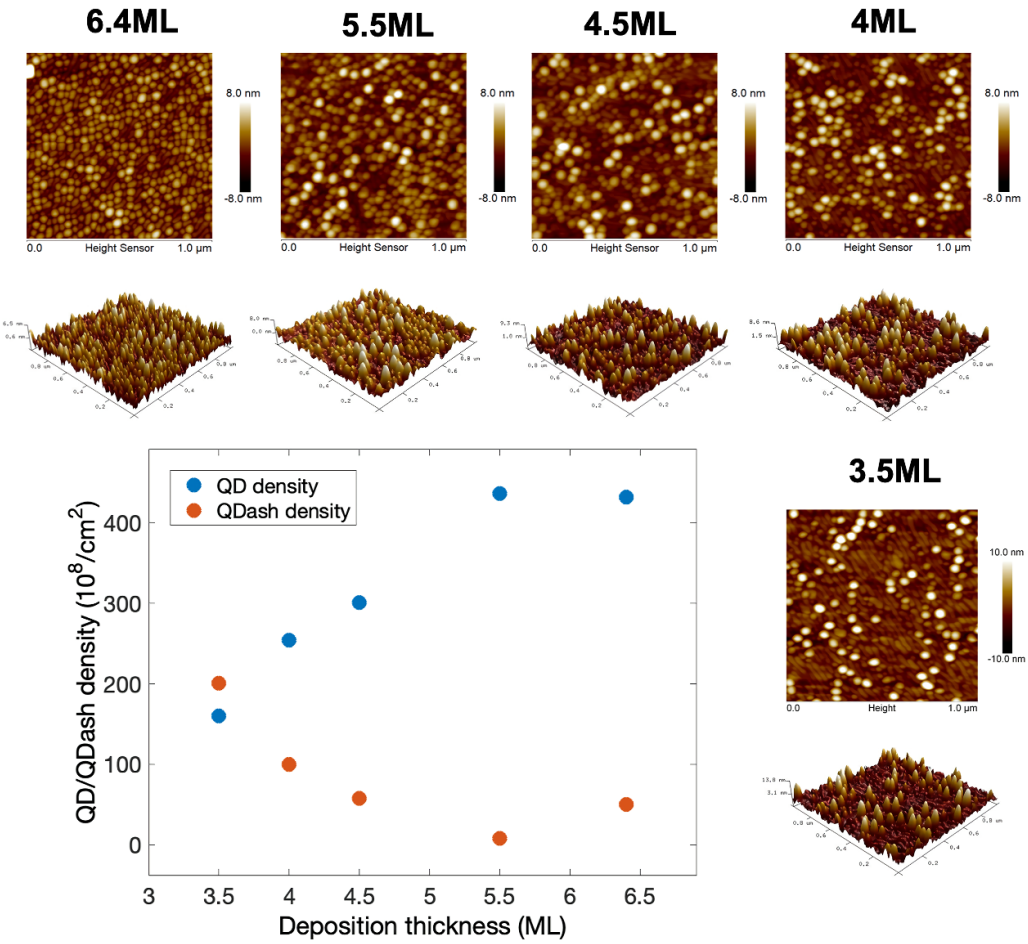

Figure 2. Morphology of InAs quantum dots with a variety of InAs deposition thicknesses ranging from 3.5 ML to 6.4 ML grown at 485 °C. Also plotted is the QD density and quantum dash (QDash) density dependence on the deposition thickness.

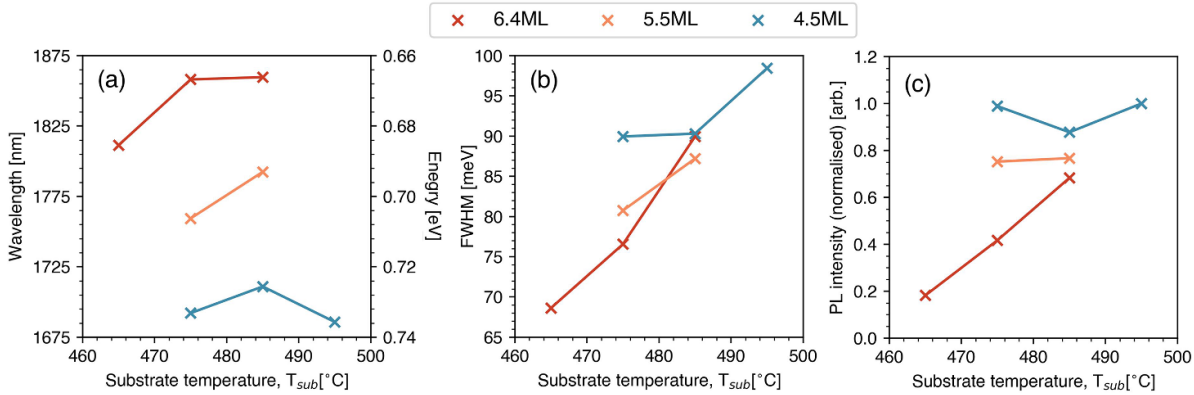

Figure 3. Photoluminescence (PL) characteristics for InAs QDs with different thicknesses. (a) Wavelengths, (b) full-width at half-maximum (FWHM) and (c) PL intensities are presented.

formation of quantum dashes is initially favoured because of the rough buffer surface and the anisotropic surface strain distribution. This growth mode is anticipated to continue until a certain thickness of InAs is deposited, causing quantum dashes to appear in more areas. However, as this process proceeds, it is evident that the surface state, including roughness, strain distribution, and nucleation site, will alter, and the consequent shift in the energy profile associated with the surface will most likely switch in favour of the second mode, i.e. QD growth, under certain growth conditions, such as the provision of As_2 rather than As_4. This is made conceivable by the elimination of the As_4-to-As_2 cracking step on the surface [4], since it substantially simplifies the bonding of In to As_2, which, in turn, reduces the anisotropic migration of In. Hence, further InAs deposition stimulates the nucleation of QDs, while simultaneously inhibiting the formation of the unfavourable quantum dashes. As expected, QD and quantum dash densities are shown to be thickness-dependent in figure 2. While the QD density increases to 436 μm^{-2}, quantum dash density decreases when just the visible dashes are considered.

Additionally, we evaluated the influence of growth temperature on the optical properties of QDs. A 635 nm continuous-wave laser with an excitation power density of 430 W cm^{-2} along with a wavelength-extended InGaAs detector was used for the RT PL measurements. The cut-off wavelength is 2 μm. As QDs are of more interest than quantum dashes, we utilised InAs with thicknesses of 4.5, 5.5, and 6.4 ML in this investigation. Figure 3 presents a summary of the results. As seen, the obtained QDs exhibit a wide diversity of PL features. (1) The emission wavelength exceeds 1.55 μm; (2) the FWHMs are significant (greater than 70 meV); (3) the PL intensities and FWHMs are approximately positively correlated with each other. All of the information presented above suggests that although we have obtained InAs nanostructures with QD shapes and a sufficiently high surface density, the resulting InAs QDs fell well short of the criterion we outlined for device application. Similarly, in [4, 7], the emission peaks of the QDs were also not positioned at 1.55 μm. As a consequence, it is essential to tailor the optical properties of InAs QDs.

The crucial step for optimised QDs is to apply the In-flush technique for growth. The In-flush technique was first established for the growth of uncoupled multi-stacked self-assembled QD layers, providing the identical surface conditions for the growth of each QD layer [21]. The In-flush technique increases the QD ensemble homogeneity in the following way: after the QD growth, a first capping layer, which is usually a material lattice-matched to InP, is deposited to partially cover the QDs. Due to the strain relaxation at the QD island top, it is not energetically favourable for adatoms to attach to [22]. Therefore, the large defective dots will be exposed while smaller dots are covered. Then the substrate temperature will be elevated, which will decompose all surface residual InAs exposed into In and As and evaporate them eventually. Ideally, after the In-flush step, as long as the thickness of the capping layer reaches a certain value, the QDs with larger height will be removed due to thermal annealing and a flat first capping layer will be obtained. Since the emission wavelength of PL is mainly determined by the height of the QDs, such In-flush growth will allow us to achieve more uniform QDs, resulting in the narrowing of PL. By carefully tuning the annealing temperature, duration, and the thickness of the capping layer, it is possible to finely control the height of the QDs with sub-nanometre precision, as will be shown by the blue-shifted PL wavelength. In our work, immediately following the formation of the intermediate QD layer with a thickness of 5.5 ML, 4 nm of $In_{0.528}Al_{0.234}Ga_{0.238}As$ was deposited at QD growth temperature to partially cap the QDs. The substrate was then raised at 30 °C min^{-1} to anneal at temperature, T_a, for 1 min. Subsequently, the remaining 96 nm $In_{0.528}Al_{0.234}Ga_{0.238}As$ layer was grown at 500 °C. Figure 4(a) depicts the structure. Due to the evaporation of the exposed top of the InAs QDs during the annealing process, more homogenous QDs were formed. Although we have altered a number of growth parameters, including the annealing temperature as well as the type, thickness and composition of the capping layer, we found that the combination of an InAlGaAs

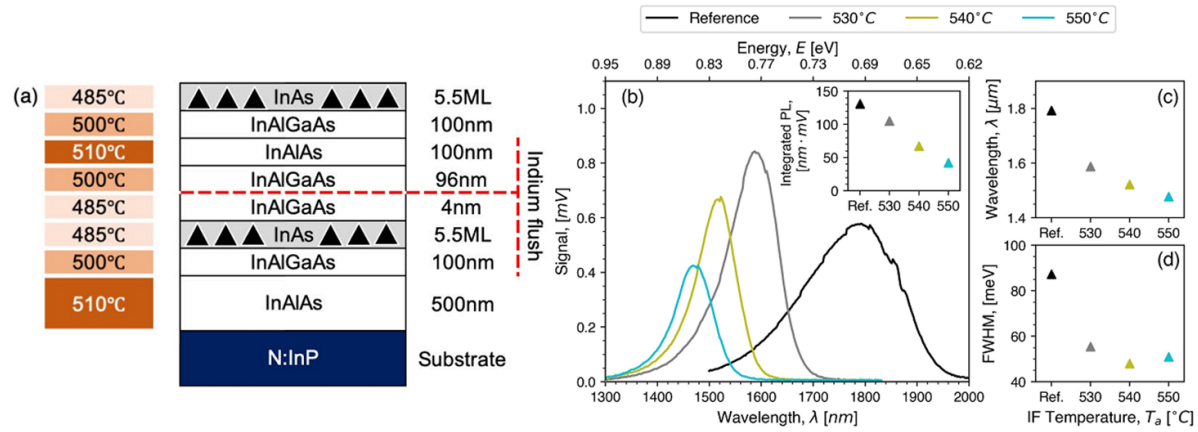

Figure 4. (a) The structure for employing the In-flush technique. (b) PL spectra of samples annealed at various growth temperatures including that of a reference without annealing. The inset shows the integrated PL intensities with annealing temperature. (c) Wavelength and (d) FWHM information are extracted from (b).

capping layer with a thickness of 4 nm and a one-minute anneal at 540 °C produced the best results. The effects of various annealing temperatures T_a on PL are shown in figures 4(b)–(d). Figure 4(b) compares the PL intensity of annealed samples with an unannealed reference sample of identical growth conditions. It can be observed that annealing at high temperatures resulted in varying degrees of the blue-shifts in the position of the PL peaks of the samples (figure 4(c)). In addition, integrated PL intensities are also shown in the inset of figure 4(b). An almost linear decrease of the integrated intensities is observed for samples annealed with increasing temperature. Considering the moderate lattice mismatch between InAs and InP, the authors believe that the majority of dots in the samples are emissive and free from crystal defects, even including some of the larger dots. Therefore, after the In-flush process, the decreased integrated PL intensity means the amount of emissive QDs is reduced, especially those emitted at large wavelengths which disappeared at annealing. A possible explanation is that during the capping layer deposition, as the island top is under strain relaxation and is not an energy-preferential site for adatom, it is likely that when the thickness of the capping layer is less than dot height, there will be an uncovered opening for these dots exposed. At high In-flush temperatures some of these larger dots will also be decomposed and evaporated completely, resulting in the reduced number of emissive QDs and thus the less integrated PL. On the other hand, the intermixing plays a role in the continued blue shift at higher annealing temperatures. Overall, the high temperature annealing is beneficial for removing point defects and impurities in the dots and for improving the dot uniformity, therefore enhanced PL intensities and narrower PL FWHM (figure 4(d)) are observed with proper In-flush annealing temperatures. Unexpectedly, the sample that we desired at 1520 nm following a blue shift from 1792 nm had the narrowest FWHM (the yellow plot in figure 4(b)), falling from 86.7 meV of the unannealed reference to 47.9 meV of this sample that was annealed at 540 °C. Additionally, this annealed sample shows a favourable peak PL intensity of 17% greater than the unannealed counterpart.

Likewise, multi-stack QD structures were also subjected to the same approach. As shown in figure 5(a), the PL peaks are consistently placed around 1.55 μm, while their FWHMs are approximately 55 meV regardless of the attempted growth conditions, in which the spacer thickness and the number of QD layers were varied, demonstrating the effectiveness and repeatability of this technique for the development of 1.55 μm InAs/InAlGaAs QDs. We also observed that the spacer layer with a thickness of (4 + 36) nm that was annealed at 540 °C exhibited the narrowest FWHM of 50.9 meV for a five-stack dot structure with the emission at 1530.2 nm (figure 5(b)). In addition, the impact of the spacer layer between each layer of QDs is evaluated on the shape of the dots (figure 5(c)). AFM results indicate that the quantum 'dots' maintain their shape up to the fifth layer, where the deposition of the quaternary compound spacer layer and the QDs underneath it do not affect the formation of upper quantum 'dots' for the structure studied. It should be pointed out that the QDs in the fifth layer are from a sample that was deliberately grown to the fifth layer of QDs and then immediately ceased growing.

It is worth mentioning that the In-flush technique first implemented in [21], is also referred to as double-cap growth, although sometimes the specifics of the height control mechanism may differ (e.g. As/P exchange rather than annealing), and is a part of the *de facto* standard for growing 1.3 μm InAs QDs on GaAs and Si currently. Correspondingly, 1.55 μm InAs QDs growth has been accomplished using the same technique for a long time. However, results on InP (001) substrates [6, 23–25], are not as impressive as those on InP (311) substrates [26, 20, 22]. This may be due to the fact that the shape of the QD on InP (001) is more or less inclined to form a quantum dash, although, on InP (311), it is not. Figure 5(d) summarises the RT FWHM values for works implementing the In-flush technique on 1.55 μm InAs QDs. It is necessary

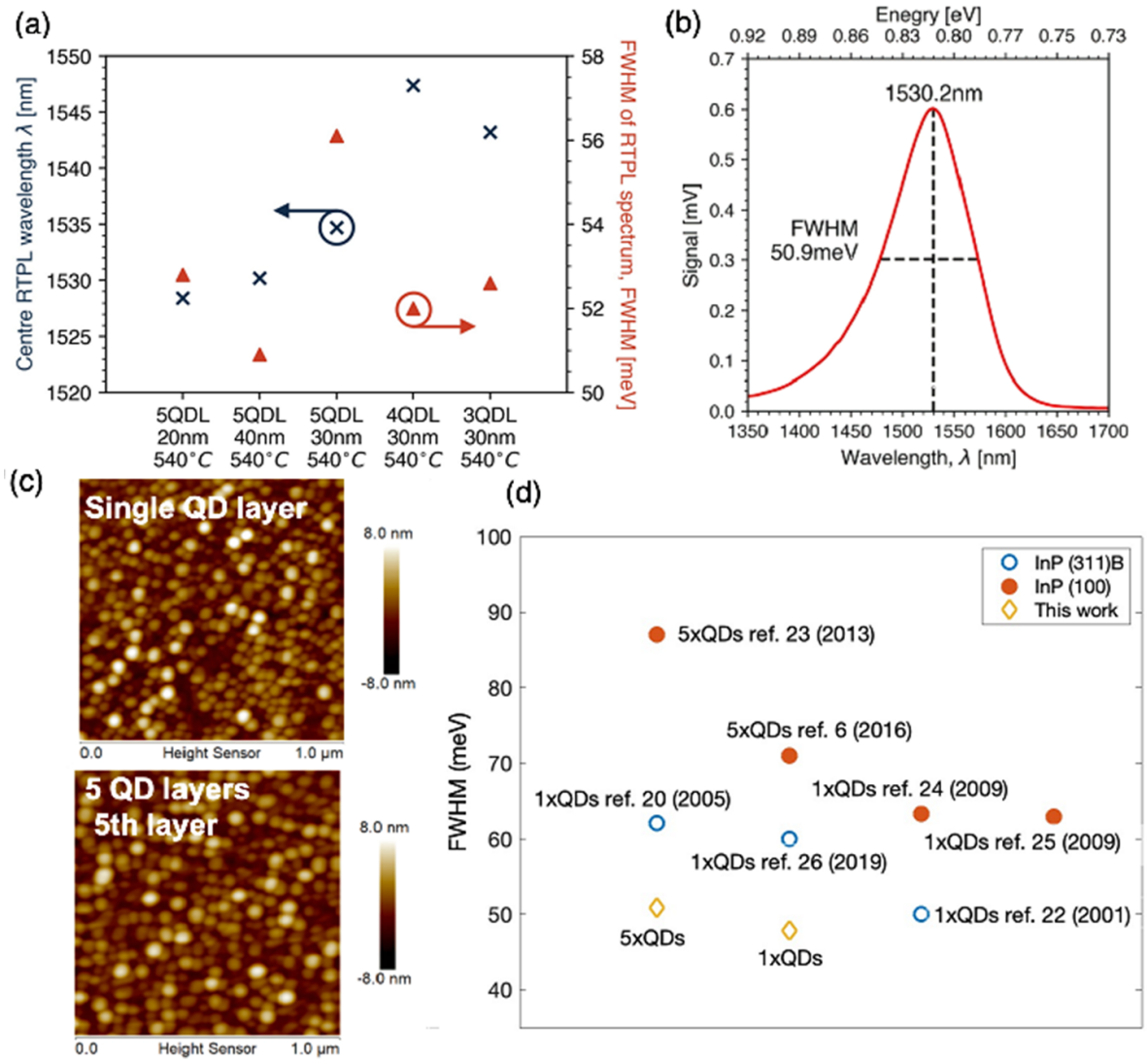

Figure 5. (a) The impact of varying the spacer thickness and the number of QDs layers on the In-flush technique samples. (b) A typical sample PL spectrum centring at 1530.2 nm with the FWHM of 50.9 meV. (c) AFM images for the morphology of the first layer QDs as well as the fifth layer QDs. (d) comparison chart of the room-temperature FWHM in our work with others that implemented the In-flush technique.

to highlight that the FWHM we obtained from the five-stack QDs structure in this paper is comparable to that of the single-layer structure on InP (311) substrate [22], whereas our single-layer sample is even narrower, suggesting, in another sense, that the QDs we obtained are more akin to the truly round-shaped 'dots' morphology rather than the quantum dashes. Therefore, we have shown that the In-flush approach can significantly increase the optical quality of the 1.55 μm InAs QDs, which may be further enhanced with optimised growth, such as digital alloy growth as shown by Kim *et al* [27], although the reproducibility of the latter remains to be verified. Additionally, we note that most PL measurements of InAs/InP QDs in the literature are performed at RT. Therefore, keeping in line with most of the available literature, we focus on RT measurements in this work, which we believe, although not as accurate as LT for measuring inhomogeneous broadening, are still sufficiently good and reliable, and more suitable for comparison with the literature than measurements performed at LT.

Lastly, we investigated low-temperature PL measurements on both single-stack and five-stack InAs QD samples. A 532 nm laser with an excitation power of 72 mW was used. The detector used was a Ge detector with a cut off wavelength of 1.85 μm. We chose to measure a five-stack sample with 30 nm thick spacers. The PL peaks of both samples, which were located around 1.55 μm when measured at RT, exhibit the anticipated blueshift to 1.4 μm at a low temperature of 10 K, coupled with an increase of PL intensity and a narrowing of FWHM (figure 6), due to the reduced thermal fluctuations in quantum confinement. The low-temperature FWHM of the single (five)-layer dots decreased from 45.3 meV (54.9 meV) to 33.7 meV (41.1 meV). Notably, at 10 K, it

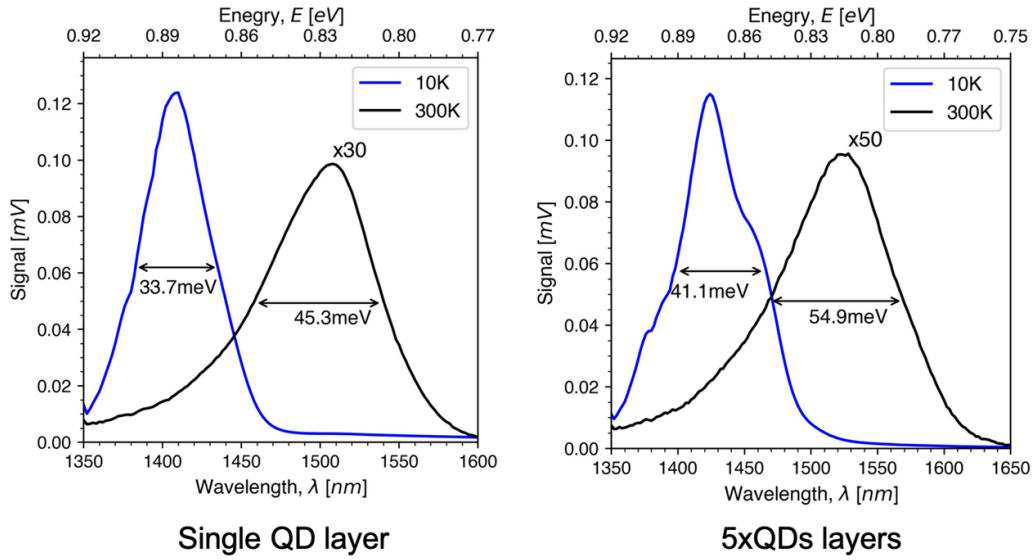

Figure 6. PL measurements at 300 K and 10 K for samples with single-stack QDs and five-stack QDs.

can be observed that the PL spectrum of the five-stack QDs is coarser compared to the single-stack QDs and can be seen to contain multiple sub-spectra. This might suggest that further work is required to improve the uniformity of the multi-stack QDs.

In conclusion, we present optically enhanced 1.55 μm InAs/InP QDs growth via appropriate growth parameters and the In-flush technique. A narrow FWHM of 50.9 meV centred at 1530.2 nm for five-stack InAs QDs was achieved with excellent reproducibility, which may be suitable for high-performance telecom laser applications.

Data availability statement

All data that support the findings of this study are included within the article (and any supplementary files).

Acknowledgments

The authors acknowledge the support of UK Engineering and Physical Sciences Research Council under Project Nos. EP/X015300/1, EP/W002302/1, EP/V029606/1, EP/T028475/1, EP/S024441/1, and EP/P006973/1.

Conflict of interest

The authors declare no conflict of interest to disclose.

Author contribution

The manuscript was written through the contributions of all authors. All authors have approved the final version of the manuscript.

ORCID iDs

Hui Jia https://orcid.org/0000-0002-8325-3948
Calum Dear https://orcid.org/0000-0003-1356-705X
Mingchu Tang https://orcid.org/0000-0001-6626-3389
Huiyun Liu https://orcid.org/0000-0002-7654-8553

References

[1] Khan M Z M, Ng T K and Ooi B S 2014 *Prog. Quantum Electron.* **38** 237
[2] Shi B, Han Y, Li Q and Lau K M 2019 *IEEE J. Sel. Top. Quantum Electron.* **25** 1–11
[3] Lenz A, Genz F, Eisele H, Ivanova L, Timm R, Franke D, Künzel H, Pohl U W and Dähne M 2009 *Appl. Phys. Lett.* **95** 203105
[4] Gilfert C, Pavelescu E-M and Reithmaier J P 2010 *Appl. Phys. Lett.* **96** 191903
[5] Banyoudeh S and Reithmaier J P 2015 *J. Cryst. Growth* **425** 299
[6] Shi B and Lau K M 2016 *J. Cryst. Growth* **433** 19
[7] Jung D, Ironside D J, Bank S R, Gossard A C and Bowers J E 2018 *J. Appl. Phys.* **123** 205302
[8] Bimberg D, Kirstaedter N, Ledentsov N N, Alferov Z I, Kop'ev P S and Ustinov V M 1997 *IEEE J. Sel. Top. Quantum Electron.* **3** 196
[9] Wu J, Chen S, Seeds A and Liu H 2015 *J. Phys. D: Appl. Phys.* **48** 363001
[10] Yu P and Wang Z M (eds) 2020 *Quantum Dot Optoelectronic Devices* (Cham: Springer)
[11] Pan S, Cao V, Liao M, Lu Y, Liu Z, Tang M, Chen S, Seeds A and Liu H 2019 *J. Semiconduct.* **40** 101302
[12] Norman J C, Jung D, Zhang Z, Wan Y, Liu S, Shang C, Herrick R W, Chow W W, Gossard A C and Bowers J E 2019 *IEEE J. Quantum Electron.* **55** 2000511
[13] Wang R H, Stintz A, Varangis P M, Newell T C, Li H, Malloy K J and Lester L F 2001 *IEEE Photonics Technol. Lett.* **13** 767
[14] Schwertberger R, Gold D, Reithmaier J P and Forchel A 2002 *IEEE Photonics Technol. Lett.* **14** 735

[15] Lelarge F *et al* 2007 *IEEE J. Sel. Top. Quantum Electron.* **13** 111
[16] Xue Y, Luo W, Zhu S, Lin L, Shi B and Lau K M 2020 *Opt. Express* **28** 18172
[17] Wan Y, Jung D, Shang C, Collins N, MacFarlane I, Norman J, Dumont M, Gossard A C and Bowers J E 2018 *ACS Photonics* **6** 279
[18] Jang J W, Pyun S H, Lee S H, Lee I C, Jeong W G, Stevenson R, Dapkus P D, Kim N J, Hwang M S and Lee D 2004 *Appl. Phys. Lett.* **85** 3675
[19] Nötzel R, Temmyo J, Kozen A, Tamamura T, Fukui T and Hasegawa H 1995 *Appl. Phys. Lett.* **66** 2525
[20] Caroff P, Bertru N, Platz C, Dehaese O, Le Corre A and Loualiche S 2005 *J. Cryst. Growth* **273** 357
[21] Wasilewski Z R, Fafard S and McCaffrey J P 1999 *J. Cryst. Growth* **201/202** 1131
[22] Paranthoen C, Bertru N, Dehaese O, Le Corre A, Loualiche S, Lambert B and Patriarche G 2001 *Appl. Phys. Lett.* **78** 1751
[23] Luo S, Ji H-M, Yang X-G and Yang T 2013 *J. Cryst. Growth* **375** 100
[24] Elias G, Létoublon A, Piron R, Alghoraibi I, Nakkar A, Chevalier N, Tavernier K, Corre A L, Bertru N and Loualiche S 2009 *Jpn. J. Appl. Phys.* **48** 070204
[25] Poole P J, Kaminska K, Barrios P, Lu Z and Liu J 2009 *J. Cryst. Growth* **311** 1482
[26] Nechay K *et al* 2019 *Appl. Phys. Lett.* **115** 171105
[27] Kim J S, Lee C-R, Choi B S, Kwack H-S, Lee C W, Sim E D and Oh D K 2007 *Appl. Phys. Lett.* **90** 153111